Simulation of a Tether of a Kite Power System Using a Lumped Mass Model

Rushdi, Mostafa. A.
Earth System Science and Technology department (ESST), Interdisciplinary Graduate School of Engineering Sciences (IGSES), Kyushu University | Faculty of Engineering and Technology, Future University in Egypt

Yoshida, Shigeo
Research Institute for Applied Mechanics (RIAM), Kyushu University

Dief, Tarek N.
Research Institute for Applied Mechanics (RIAM), Kyushu University

https://doi.org/10.15017/1960663

出版情報：Proceedings of International Exchange and Innovation Conference on Engineering & Sciences (IEICES). 4, pp.42-47, 2018-10-18. 九州大学大学院総合理工学府
バージョン：
権利関係：

Simulation of a Tether of a Kite Power System Using a Lumped Mass Model

Mostafa. A. Rushdi[1], Shigeo Yoshida[2], Tarek N. Dief[2]
[1]Earth System Science and Technology department (ESST), Interdisciplinary Graduate School of Engineering Sciences (IGSES), Kyushu University, Japan | Faculty of Engineering and Technology, Future University in Egypt.
[2]Research Institute for Applied Mechanics (RIAM), Kyushu University, Japan.
[1]rushdimostafa@riam.kyushu-u.ac.jp / Mostafa.Roshdi@fue.edu.eg

Abstract: *This paper introduces a new approach of harvesting energy from wind using a Kite Power System (KPS). Kite power systems are targeted herein because they have many advantages over other renewable energy sources, especially those related to wind energy. We capture the essential features of the tether connected to the kite via a lumped mass model and calculate the aerodynamic forces which cause tension in the tether. Work exerted by the tensile force in the tether is converted to electric power using a specially-designed generator. We present a detailed mathematical analysis of the system followed by typical simulation results.*

Keywords: Kite power system; Wind energy; Lumped mass model.

1. INTRODUCTION

Airborne Wind Energy (AWE) is a prominent form of renewable energy [1-14] that denotes the generation of usable power by airborne devices [9, 13, 14]. AWE systems constitute a novel way to harvest wind energy at higher altitudes without the need of a heavy tower and sophisticated constructions. In contrast to towered wind turbines, AWE systems are either flying freely in the air, or are mechanically connected to the ground, like tethered kites or tethered balloons. However, all AWE systems with significant power output belong to the second type (i.e., are connected to the ground), which allows an exploitation of the relative velocity between the airmass and the ground. The prominent reasons for particular use of AWE in electricity production are (a) AWE systems reach winds blowing at higher-altitude atmospheric layers that are inaccessible by traditional wind turbines. These winds are typically stronger and more consistent than those close to the ground, (b) the area that can be swept by an AWE system is not tightly limited, unlike that of a turbine which is limited by its diameter, and hence an AWE system is inherently more efficient, and (c) AWE systems are expected to need less material investment per unit of usable power than most other renewable energy sources. An important share of the worldwide primary energy could be potentially extracted from high-altitude winds. Two prominent AWE system architectures are Ground-Gen systems in which the conversion of mechanical energy into electrical energy takes place on the ground and Fly-Gen systems in which such conversion is done on the flying object [14].

A kite constituting an AWE system is an ingeniously engineered airfoil having high-tech tethers that are fifteen times as strong as steel. A tether is a rope to tie something to a post or other fixed place, usually so that it can move freely within a small area. Understanding tether dynamics is extremely complex with numerous factors effecting the behavior of a cable – from the shape and aerodynamics of the tether to the elasticity, bending and torsion of the materials used, not to mention the changing wind speed and temperature at heights of up to 20 km. There are many scholarly papers exploring energy harvesting by tethered kites [15-34]. However, very few established design guidelines for AWE systems currently exist [35].

In this paper, we employ a Lumped Mass Model (LMM), also called lumped element (mass-spring-damper) model) for the tether-kite system. This model secures a simplified description of the behavior of such a spatially-distributed mechanical system by assuming that distributed masses are lumped (concentrated as point rigid bodies) [36-38]. This simplification reduces the state space of the system to a finite dimension, and the partial differential equations (PDEs) of the continuous (infinite-dimensional) time and space model of the original system into ordinary differential equations (ODEs) with a finite number of parameters.

The remainder of this paper is organized as follows: Section 2 presents the lumped mass model for the tether. Section 3 consists of the mathematical equations for the lumped mass model of the tether connected to a kite and explains how this model is simulated. Section 4 presents numerical results and data analysis. Section 5 concludes the paper, and outlines our plans for future work.

2. LUMPED MASS MODEL

To aid in the cable modelling [36-38], an inertial reference frame and a sequence of moving frames attached at points along the cable are introduced. The inertial reference frame (X_G, Y_G, Z_G) is fixed at the surface. The horizontal direction, X_G, is defined positive to the right, the vertical direction, Z_G, is defined positive upward, and the Y_G direction completes a right-handed coordinate system [30]. The armoured cable is discretized into an assembly of N linear elements. The mass of the cable is lumped at the N +1 node points, 0 to N (see Fig. 1). The kite is situated at the end of the tether (at node N+1) and the kite control unit (KCU) is placed at node N−1 (see Fig. 2). Their masses constitute additional masses at these two nodes. To model the elasticity of the true cable, each visco-elastic cable element is idealized as a parallel combination of an ideal spring and a viscous damper [26]. This typical

mass-spring-damper system is described by the standard 2nd-order ODE:

$$\frac{d^2x}{dt^2} + 2\,\xi\,\omega_n \frac{dx}{dt} + \omega_n^2 x = 0 \qquad (1)$$

where

$$\xi = \frac{c}{2\sqrt{mk}} \quad \text{and} \quad \omega_n = \sqrt{\frac{k}{m}} \qquad (2)$$

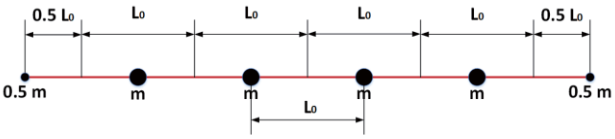

Figure 1. Illustration of mass distribution for LLM of 5 lumps.

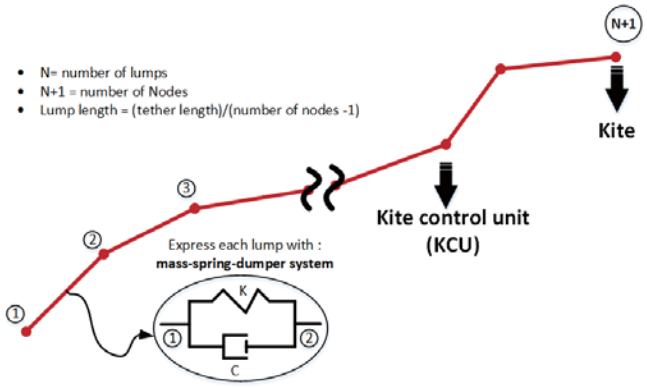

Figure 2. Schematic illustration of the lumped mass model of the tether-kite system.

Note that the word "Node" as indicated by a black circle in Fig. 1, has lumped mass of the tether, position, velocity which will be differentiated to get acceleration. But the "lump" will be the length between two successive nodes, it indicates the geometry of the tether, so we calculate the fluid forces at the lump.

3. MATHEMATICAL EQUATIONS AND SIMULATION

In this section, we illustrate the mathematical equations which describe the LMM for the tether-kite system. An overview of the simulation procedures is shown in Figure.3.

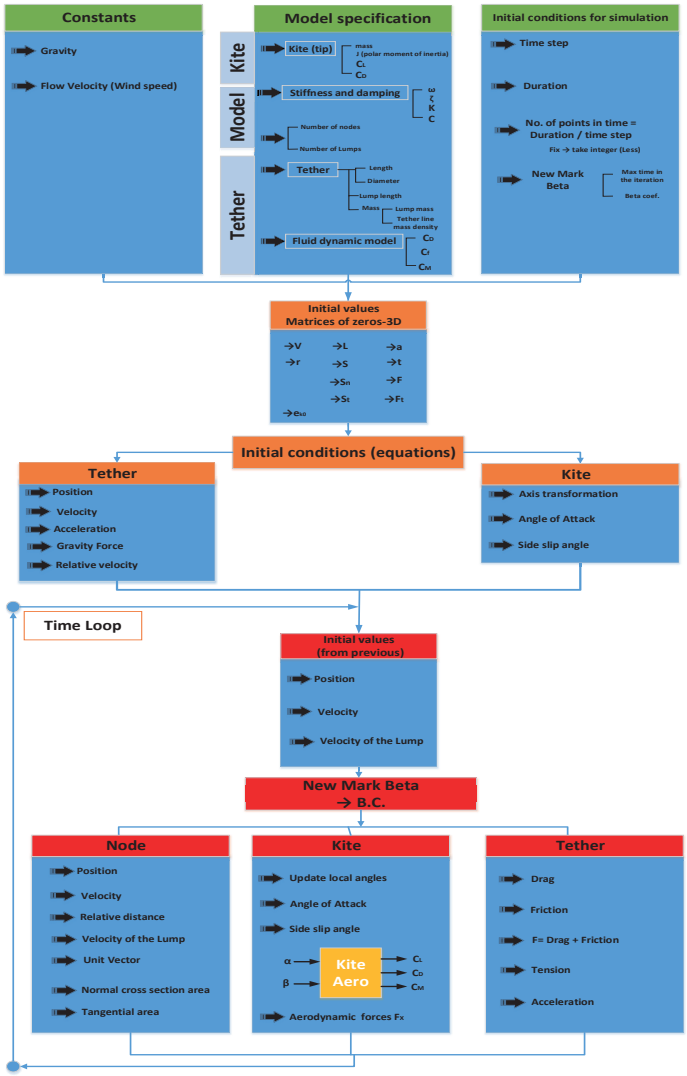

Figure 3. Overview of the simulation procedure.

3.1 Initial conditions (equations)

The tether-kite system has two frames connected with three angles (rolling – pitching – yawing).

$$\boldsymbol{\phi}_G^k = [\phi \quad \theta \quad \psi]^T \qquad (3)$$

Where $\boldsymbol{\phi}_G^k$ indicates the angles of kite in the global axis, hence that the kite at node N+1 ($\boldsymbol{\phi}^k = \boldsymbol{\phi}^{N+1}$). We assume at the beginning that there is no rotation in axes (motion is purely translational), so that the angles of kite in the local axis $\boldsymbol{\phi}_l^k$ will be the same in the global axis

$$\boldsymbol{\phi}_l^k = \boldsymbol{\phi}_G^k \qquad (4)$$

Then we have to initiate some values for the tether and the kite as indicated in the following subsections.

3.1.1 The Tether

The tether length (L_T) is discretized to lumps with lump length (L_0) which are connected by nodes. Calculations are done at each node, *i.e.*, N+1 times.

- **Position:** Simple resolution of each lump in global axis (see Fig. 4) results in

$$\boldsymbol{r}^j = \boldsymbol{\ell}\,[\cos(\theta) \quad 0 \quad -\sin(\theta)]^T \qquad (5)$$

where $\boldsymbol{r}^j$ indicates position of the j[th] node, and

$$\ell = \frac{N-1}{(N+1)-1} L_T \qquad (6)$$

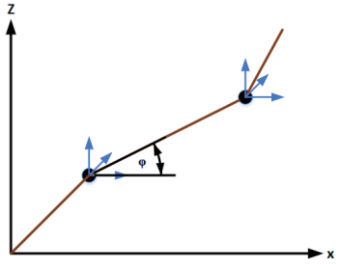

Figure 4. At the beginning of each lump, we put a new origin for the axis and then take the resolution.

- **Velocity:**

$$\boldsymbol{V}^j = \frac{dr}{dt} = \frac{dr}{d\theta}\frac{d\theta}{dt} \qquad (7)$$

As initial case $\frac{d\theta}{dt} = \frac{2\pi}{L_T}$

- **Acceleration:**

$$\boldsymbol{a}^j = g \qquad (8)$$

- **Gravity force** (see Fig. 6)**:**

$$\boldsymbol{F_g} = m^j g \qquad (9)$$

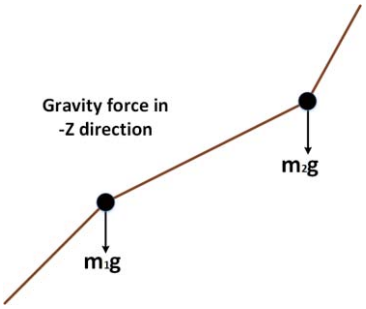

Figure 5. Gravity force in -ve direction.

- Relative velocity at each lump (see Fig. 6)

$$\boldsymbol{V}_{rel}^j = \boldsymbol{V}_0^j - \boldsymbol{V}^j \qquad (10)$$

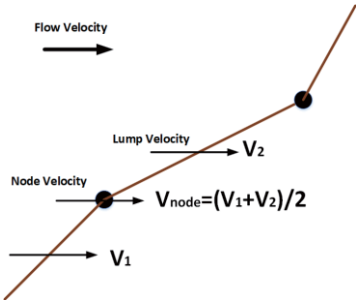

Figure 6. Illustration of the velocity directions

- Relative velocity at each node:
  The average of two successive $\boldsymbol{V}_{rel}^j$

3.1.2 The Kite

The kite will be at the end of the tether (the final lump at node N+1). For simplicity, it is treated as rigid wing with NACA 4418 airfoil.

- **Rotation of kite**

$$[\boldsymbol{R}^k] = [\boldsymbol{R}(\emptyset, \theta, \psi)]$$

where, $[\boldsymbol{R}(\emptyset, \theta, \psi)]$ is the rotation matrix.

- **Unit vector with the kite (in global axis)**

$$[\boldsymbol{e}^k] = [\boldsymbol{R}^k]\,[\boldsymbol{e}_0^k] \qquad (11)$$

where, $[\boldsymbol{e}_0^k]$ is a unit matrix.

- **Angle of attack:** is defined by the 2 vectors of the relative velocity and a unit vector attached to the kite *via* the dot product (Fig. 7).

$$\alpha^k = \pi - cos^{-1}\left(\frac{\boldsymbol{e}_x^k \odot \boldsymbol{V}_{rel}^j}{\|\boldsymbol{V}_{rel}^j\|\|\boldsymbol{e}_x^k\|}\right) \qquad (12)$$

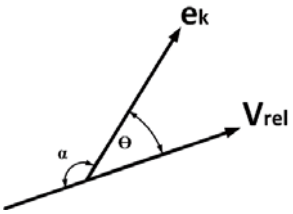

Figure 7. Illustration of the angle-of-attack (AOA) formula as a dot product definition.

- **Side slip angle:** We assume that the kite is flying directly to the flow velocity vector, so all over the simulation we consider $\beta = 0$.

- **Aerodynamic coefficients:** As we said before, the kite will be treated as rigid wing with NACA 4418 airfoil. Figures 10 and 11 show the data of $(C_L - \alpha)$ and $(C_D - \alpha)$ curves in the range of $-20^0 < \alpha < 20^0$ and we extrapolate the curves up to 180^0 and -180^0 with a function of sines and cosines. So, we build a function containing the data of the airfoil. Subsequently, we calculate the angle of attack "α", and read C_L and C_D implied by the extrapolated curves.

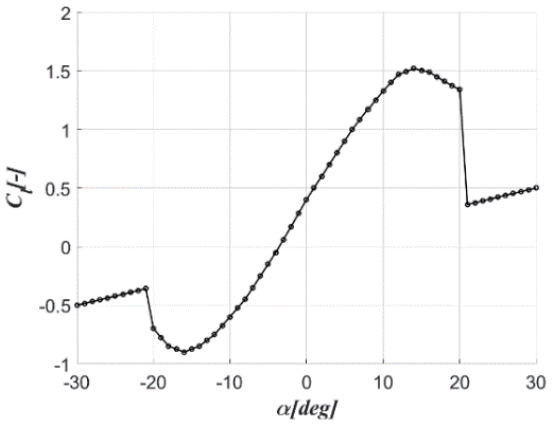

Figure 8. $C_L - \alpha$ curve for NACA 4418.

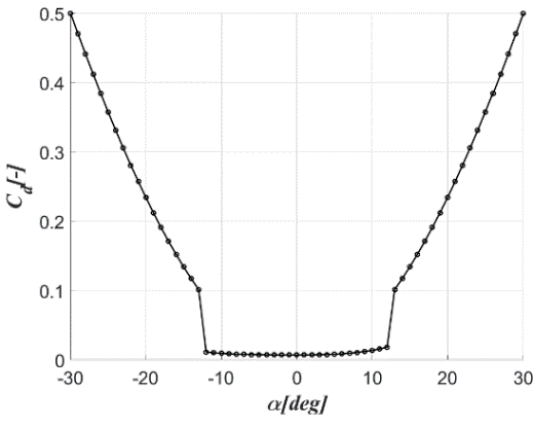

Figure 9. $C_D - \alpha$ curve for NACA 4418.

3.2 Time Loop

After the initialization section, we calculate all values again at each time step. The dummy counter on time is "i" starting from 2 till the total number of points in time and the initial values are taken from previous calculations. We use the New-Mark Beta formulas for numerical integration of differential equations, with beta coefficient = 1/6.

$$\dot{\boldsymbol{u}}_{n+1} = \dot{\boldsymbol{u}}_n + \frac{\Delta t}{2}(\ddot{u}_n + \ddot{u}_{n+1})$$

$$\boldsymbol{u}_{n+1} = \boldsymbol{u}_n + \Delta t\, \dot{\boldsymbol{u}}_n + \frac{1-2\beta}{2}\Delta t^2\, \ddot{u}_n + \beta\, \Delta t^2\, \ddot{\boldsymbol{u}}_{n+1}$$

The velocity and position at the beginning are set to zero as a boundary condition. Now we consider the calculation of the three angles. First, we assume that there is no rolling (around X_G-axis), so as to ensure that the kite will not hit the tether.

$$\boldsymbol{\phi}_G^k(\mathrm{i},1) = 0 \qquad (13)$$

The pitching angle (around the Y_G-axis) is given by

$$\boldsymbol{\phi}_G^k(\mathrm{i},2) = -\sin^{-1}\left(\frac{\boldsymbol{r}_z^j}{\left\|\boldsymbol{V}_{rel}^j(x,y,z)\right\|}\right) \qquad (14)$$

The yawing angle (around the Z_G-axis) is given by

$$\boldsymbol{\phi}_G^k(\mathrm{i},3) = -\sin^{-1}\left(\frac{\boldsymbol{r}_y^j}{\left\|\boldsymbol{V}_{rel}^j(x,y)\right\|}\right) \qquad (15)$$

3.2.1 The Lumps

We calculate the following at each lump, because it is geometry related, using the counter j from 1 to the number of lumps "N"

- Relative distance

$$L^j = \left\|\boldsymbol{r}^{j+1} - \boldsymbol{r}^j\right\| \qquad (16)$$

- Velocity

$$\boldsymbol{u}^j = \frac{L^j - L_s^j}{\Delta t} \qquad (17)$$

- Unit vector

$$\boldsymbol{dir}^j(1\to 3) = \frac{\boldsymbol{r}^{j+1} - \boldsymbol{r}^j}{L^j} \qquad (18)$$

- Normal cross section area

$$S_n^j = L^j d \qquad (19)$$

- Tangential area

$$S_t^j = \pi\, d\, L^j \qquad (20)$$

3.2.2 The Kite

Again, we calculate the angle of attack (AOA) as in Sec 3.1.2, and then evaluate the aerodynamic forces

$$F_x^k(i,1\to 3) = \frac{1}{2}\rho\|V_x\|^2 S^k C_{a0}(i,1\to 3) \qquad (21)$$

The index k = 1 denotes the lift force with the corresponding $C_{a0} = C_L$, k = 2 depicts the drag with corresponding $C_{a0} = C_D$ and finally k = 3 refers to the moment with corresponding $C_{a0} = C_M$.

3.2.3 The Tether

The fluid force at each lump is calculated using counter j from 1 to the number of lumps "N"

- Drag (normal to the axis of the tether)

$$F_D^j = \frac{1}{2}C_D\rho S_t\left|\boldsymbol{V}_{rel}^j \odot \boldsymbol{dir}^j\right|\left|\boldsymbol{V}_{rel}^j \odot \boldsymbol{dir}^j\right| \qquad (22)$$

- Drag (parallel to the axis of the tether)

$$F_f^j = \frac{1}{2}C_f\rho S_n\left|\boldsymbol{V}_{rel}^j - (\boldsymbol{V}_{rel}^j \odot \boldsymbol{dir}^j)\boldsymbol{dir}^j\right| \cdot * \boldsymbol{V}_{rel}^j \qquad (23)$$

- Total force in each lump

$$\mathrm{F}^j = F_D^j + F_f^j \qquad (24)$$

- Tension in each lump

$$\mathrm{T} = -\mathrm{K} * \max\begin{cases} L^j - L_0^j - C\,\boldsymbol{u}^j\boldsymbol{dir}^j \\ 0 \end{cases} \qquad (25)$$

Equation (25) expresses the tensile force in the tether that is transferred to the generator so as to be converted into electricity.

4. RESULTS

We produced extensive results through our detailed simulation the tether-kite system. Samples of our results are displayed in Figs. 10-14. The simulation covered the tether and kite positions at every single point in time, the variation of angles related to each other and with time, and the forces versus time. This is our first cut at the problem and does not include many potential en enhancements such as maximizing the tension and the power generated or controlling the motion of the kite.

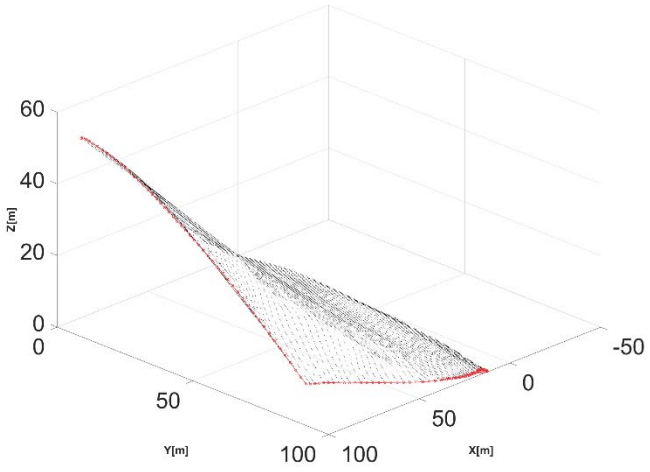

Figure 10. 3D drawing of the tether-kite system simulation.

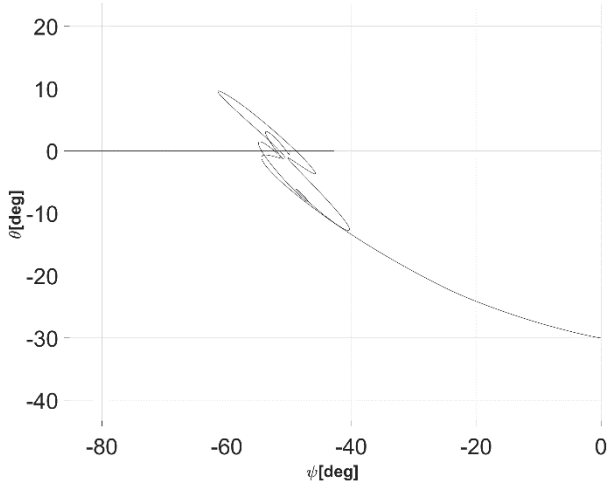

Figure 11. Variation of yawing versus pitching angles.

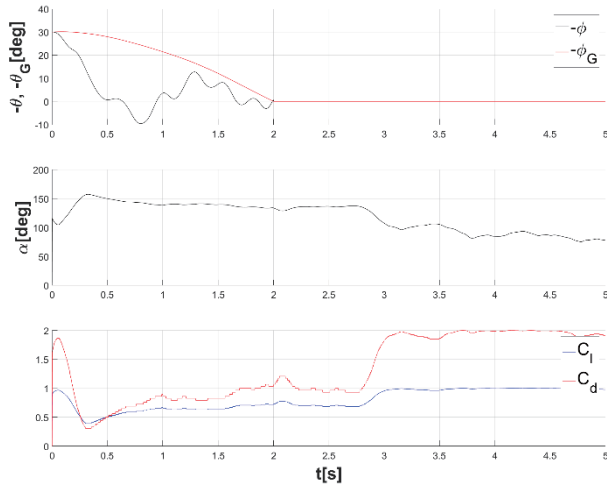

Figure 12. Angles and aerodynamic variations with time.

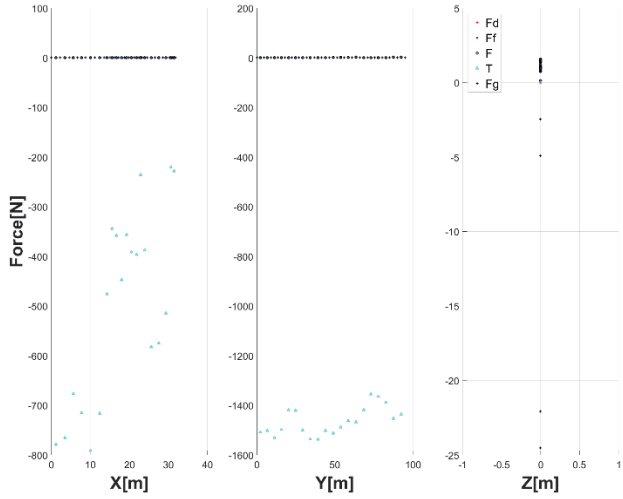

Figure 13. Forces in the 3 directions.

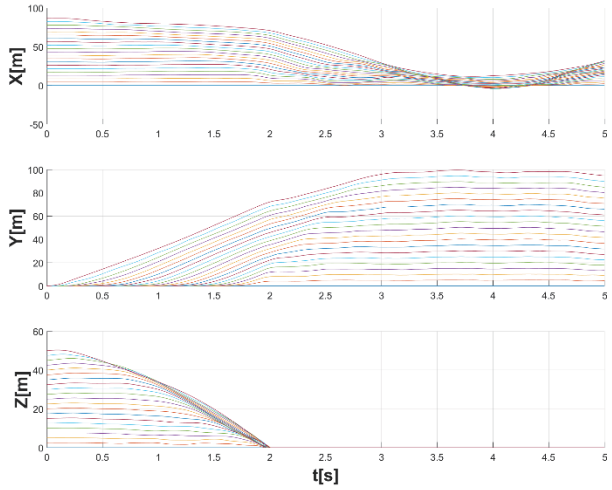

Figure 14. Variation of each lump position with time

We also make a validation for the characteristics of the kite. We deduce the effect of horizontal relative motion on the angle of attack (AOA). If we move the kite upward to the right, then using simple geometry (see Fig. 16), we calculate the change of the angle of attack as

$$\Delta\alpha = \tan^{-1}\left(\frac{\Delta r_z^j}{Vx_{rel}^j - \Delta Vx_{rel}^j}\right)$$

$$\Delta r_z^j = r_z^j(i) - r_z^j(i-1)$$

$$\Delta Vx_{rel}^j = Vx_{rel}^j(i) - Vx_{rel}^j(i-1)$$

Then we set $\alpha = \theta + \Delta\alpha$, and drew it with C_l and C_D. This is supposed to be like the input data approximately.

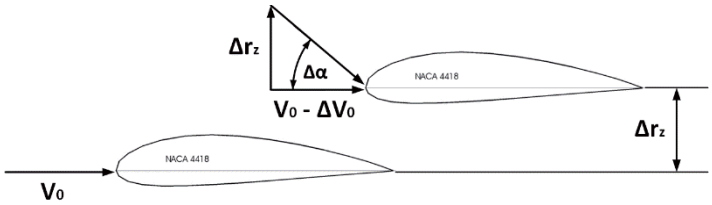

Figure 15. Illustration of AOA variation.

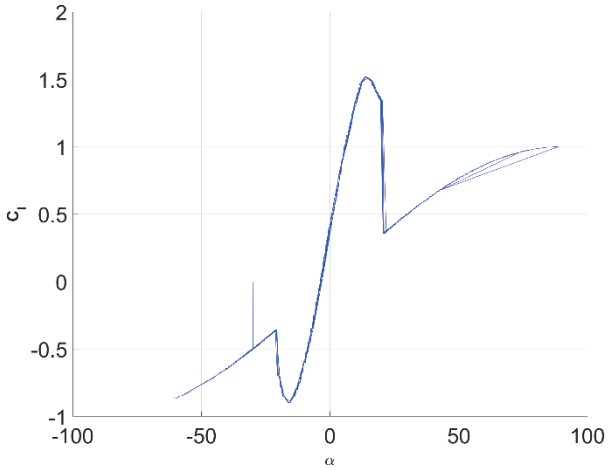

Figure 16. $C_l - \alpha$ curve generated from code for validation

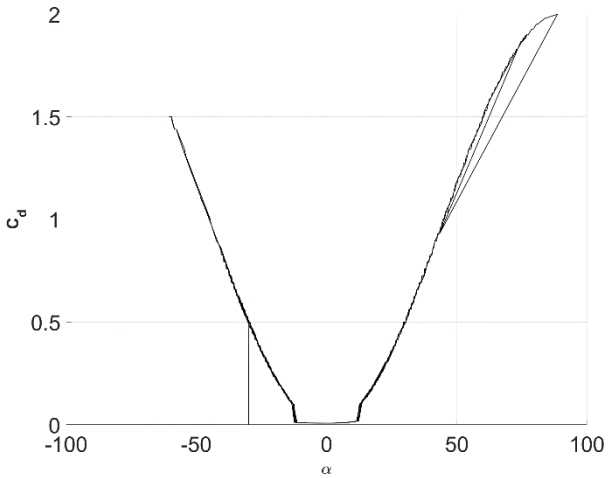

Figure 17. $C_D - \alpha$ curve generated from code for validation.

5. CONCLUSIONS

This paper studied a Kite Power System (KPS) by modeling the tether connected to the kite as a lumped mass model and calculating the aerodynamic forces which cause tension in the tether. Detailed mathematical analysis of the system is given and typical simulation results are obtained and discussed.

Our own future work focuses on finding the *optimal* path for the kite to *maximize* its power output. The ideal kite trajectory is known to resemble the *figure of number eight*. Therefore, we plan to explore control solutions of our tether-kite system which might generate this ideal path. Subsequently, we strive to confirm our theoretical findings experimentally by building a *Kite Control Unit* (KCU) which controls the movement of the kite by controlling the tension in the tether. Other lines of future explorations include pursuing an *optimization* framework based on a differentiable model for *varying-length* tether dynamics. Another innovative extension of the single-kite system is called the *laddermill*, in which *several* kites are deployed to high altitudes by means of a single cable connected to a drum on the ground station. The individual kites and ground stations have to communicate among themselves to avoid collisions and to optimize the total power output.

Acknowledgment

The authors are greatly indebted to their dear colleague Dr. Makoto Sueyoshi for providing a preliminary code on which the LMM code used herein is based.

6. REFERENCES

[1] Popper, S. W., Lempert, R. J., & Bankes, S. C. (2005). Shaping the future. *Scientific American*, *292*(4), 66-71.

[2] Boyle, C., & Coates, G. T. K. (2005). Sustainability principles and practice for engineers, *IEEE Technology and Society Magazine*, 24(3): 32-39.

[3] Dincer, I. (2000). Renewable energy and sustainable development: a crucial review. *Renewable and Sustainable Energy Reviews*, *4*(2), 157-175.

[4] Anastas, P. T., & Zimmerman, J. B. (2003). Design through the twelve principles of green engineering. Environmental Science and Technology, 37: 94A-101A.

[5] Rushdi, A. M. A. (2009). Engineering thinking on exploring the future. *Journal of King Abdulaziz University: Engineering Sciences*, *20*(2), 111-140.

[6] Barai, M. K., & Saha, B. B. (2015). Energy security and sustainability in Japan. *Evergreen, Joint Journal of Novel Carbon Resource Sciences & Green Asia Strategy*, *2*(1), 49-56.

[7] Cherp, A., & Jewell, J. (2011). The three perspectives on energy security: intellectual history, disciplinary roots and the potential for integration. *Current Opinion in Environmental Sustainability*, *3*(4), 202-212.

[8] Kucharski, J., & Unesaki, H. (2016). Energy security and sustainability in Japan. *International Journal of Sustainable Future for Human Security*, (4)1, 2-10.

[9] Diehl, M. (2013). Airborne Wind Energy: Basic Concepts and Physical Foundations. Chapter 1 in *Airborne Wind Energy* (pp. 3-22). Springer, Berlin, Heidelberg.

[10] Lunney, E., Ban, M., Duic, N., & Foley, A. (2017). A state-of-the-art review and feasibility analysis of high altitude wind power in Northern Ireland. *Renewable and Sustainable Energy Reviews*, *68*, 899-911.

[11] Halawa, A. M., Elhadidi, B., & Yoshida, S. (2018). Aerodynamic performance enhancement using active flow control on du96-w-180 wind turbine airfoil. *Evergreen, Joint Journal of Novel Carbon Resource Sciences & Green Asia Strategy*, *5*(1), 16-24.

[12] Ismaiel, A. M. M., & Yoshida, S. (2018). Study of turbulence intensity effect on the fatigue lifetime of wind turbines. *Evergreen: Joint Journal of Novel Carbon Resource Sciences & Green Asia Strategy*, *5*(1), 25-32.

[13] Fagiano, L., & Milanese, M. (2012, June). Airborne wind energy: An overview. In *American Control Conference (ACC), 2012* (pp. 3132-3143). IEEE.

[14] Cherubini, A., Papini, A., Vertechy, R., & Fontana, M. (2015). Airborne wind energy systems: A review of the technologies. *Renewable and Sustainable Energy Reviews*, *51*, 1461-1476.

[15] Bauer, F., Kennel, R. M., Hackl, C. M., Campagnolo, F., Patt, M., & Schmehl, R. (2018). Drag power kite with very high lift coefficient. *Renewable Energy*, *118*, 290-305.

[16] Bigi, N., Nême, A., Roncin, K., Leroux, J. B., Bles, G., Jochum, C., & Parlier, Y. (2018). Analytical Tether Model for Static Kite Flight. In *Airborne Wind Energy* (pp. 57-78). Springer, Singapore.

[17] Canale, M., Fagiano, L., Ippolito, M., & Milanese, M. (2006, December). Control of tethered airfoils for a new class of wind energy generator. In *Decision and Control, 2006 45th IEEE Conference on* (pp. 4020-4026). IEEE.

[18] Canale, M., Fagiano, L., & Milanese, M. (2007). Power kites for wind energy generation: Fast predictive control of tethered airfoils. *IEEE Control Systems Magazine*, *27*(6), 25-38.

[19] Costello, S., François, G., & Bonvin, D. (2013). Real-time optimization for kites. Proceedings of the 5th IFAC International Workshop on Periodic Control Systems, The International Federation of Automatic Control, Caen, France, pp. 64-69.

[20] Fechner, U. (2016). A Methodology for the Design of Kite-Power Control Systems. Unpublished PhD Thesis, Delft University of Technology, Delft, the Netherlands.

[21] Linskens, H. T. K., & Mooij, E. (2016). Tether dynamics analysis and guidance and control design for active space-debris removal. *Journal of Guidance, Control, and Dynamics*, 39(6), 1232-1243.

[22] Milutinović, M., Kranjčević, N., & Deur, J. (2014). Multi-mass dynamic model of a variable-length tether used in a high altitude wind energy system. *Energy conversion and management*, *87*, 1141-1150.

[23] Pastor-Rodríguez, A., Sánchez-Arriaga, G., & Sanjurjo-Rivo, M. (2017). Modeling and stability analysis of tethered kites at high altitudes. *Journal of Guidance, Control, and Dynamics*, *40*(8), 1892-1901.

[24] Sánchez-Arriaga, G., Pastor-Rodríguez, A., Borobia-Moreno, R., & Schmehl, R. (2018, June). A constraint-free flight simulator package for airborne wind energy systems. In *Journal of Physics: Conference Series* (Vol. 1037, No. 6, p. 062018). IOP Publishing.

[25] Smoot, S., & Kroo, I. (2011). Dimensional analysis and scaling for tethered lifting bodies. In *11th AIAA Aviation Technology, Integration, and Operations (ATIO) Conference*, (AIAA-2011-6907), 1-15.

[26] Thorpe, D. (2011). Modelling and Control of Tethered Kite Systems for Wind Energy Extraction. Unpublished PhD Thesis, RMIT University, Melbourne, Victoria, Australia.

[27] Williams, P., Lansdorp, B., & Ockesl, W. (2008). Optimal crosswind towing and power generation with tethered kites. *Journal of Guidance, Control, and Dynamics*, *31*(1), 81-93.

[28] Williams, P., Lansdorp, B., & Ockels, W. (2008). Nonlinear control and estimation of a tethered kite in changing wind conditions. *Journal of Guidance, Control, and Dynamics*, *31*(3), 793-799.

[29] Buckham, B. J. (2003). Dynamics modelling of low-tension tethers for submerged remotely operated vehicles. Unpublished PhD Thesis, University of Victoria, Victoria, British Columbia, Canada.

[30] Dief, T. N., Rushdi, M. A. & Yoshida, S. (2018, June). Modeling and control of a kite power system, Grand Renewable Energy (GRE) Conference, Tokyo, Japan.

[31] Canale, M., Fagiano, L., & Milanese, M. (2010). High altitude wind energy generation using controlled power kites. *IEEE Transactions on Control Systems Technology*, 18(2), 279-293.

[32] Gros, S., & Diehl, M. (2013). Modeling of Airborne Wind Energy Systems in Natural Coordinates. Chapter 10 in *Airborne Wind Energy* (pp. 181-203). Springer, Berlin, Heidelberg.

[33] Lansdorp, B., & Williams, P. (2006). The laddermill: Innovative wind energy from high altitudes in Holland and Australia. *Windpower 2006*, Adelaide, Australia.

[34] Fechner, U., & Schmehl, R. (2012, October). Design of a distributed kite power control system. In *Control Applications (CCA), 2012 IEEE International Conference on* (pp. 800-805).

[35] Fagiano, L., & Marks, T. (2015). Design of a small-scale prototype for research in airborne wind energy. *IEEE/ASME Transactions on Mechatronics*, 20(1), 166-177.

[36] Mooi, H. G., & Huibers, J. H. A. M. (2000). Simple and effective lumped mass models for determining kinetics and dynamics of car-to-car crashes. *International Journal of crashworthiness*, 5(1), 7-24.

[37] Fonfach, J. M., Manderbacka, T., & Neves, M. A. S. (2016). Numerical sloshing simulations: Comparison between Lagrangian and lumped mass models applied to two compartments with mass transfer. *Ocean Engineering*, 114, 168-184.

[38] Reichl, K. K., & Inman, D. J. (2017). Lumped mass model of a 1D metastructure for vibration suppression with no additional mass. Journal of Sound and Vibration, 403, 75-89.